Eur. Phys. J. Plus (2015) **130**: 60
DOI 10.1140/epjp/i2015-15060-2

THE EUROPEAN PHYSICAL JOURNAL PLUS

Regular Article

Ab initio study of vibrational and optical properties of stable Zn_mO_n (m + n = 2 to 5) nanoclusters

P.S. Yadav[a], D.K. Pandey[b], S. Agrawal, and B.K. Agrawal

Department of Physics, University of Allahabad, Allahabad - 211002, India

Received: 24 July 2014 / Revised: 9 February 2015
Published online: 2 April 2015 –

Abstract. An *ab initio* study has been performed for the various properties of the most stable configuration out of the various configurations having "m" number of Zn and "n" number of O atoms *i.e.* Zn_mO_n ($m + n$ = 2 to 5) nanoclusters by employing B3LYP-DFT/6-311G(3df) method. We report here the vibrational frequencies, IR intensities, Rel IR intensities, Raman scattering activities and optical absorption for these nanoclusters. The structure having minimum energy out of all the configurations having similar values of "m" and "n" is considered as the most stable. We found that all the different configurations of ZnO_4, Zn_2O_3 and Zn_4O complexes are not stable because they possess at least one vibrational frequency which is imaginary. The high vibrational frequencies of each nanocluster arise from the symmetrical and asymmetrical stretching vibrations whereas the lower frequencies belong to the wagging, rocking and the out-of-plane vibrations of Zn and O atoms. Our predicated results for the most intense minimum excitation energies of the ZnO and Zn_2O_2 nanoclusters exhibit excellent agreement with the available experimental data. All the nanoclusters show strong absorption in the ultraviolet region but some also exhibit weak absorption in the visible region.

1 Introduction

For more than two decades, semiconductor nanostructure materials have been widely studied because of their potential applications in electronics, optics and photonics. A nanocluster is an intermediate phase between molecule and bulk [1,2]. In nanoclusters, the surface area-to-volume ratio is quite high as compared to bulk [3,4]. Semiconductor nanoclusters have attracted immense attention as their electronic and optical properties show important changes from their corresponding bulk properties due to the quantum confinement effect. Among II-VI compounds, ZnO is a direct band gap semiconductor with a large band gap of 3.37 eV and a large exciton binding energy of 60 meV. Nanostructured ZnO has been recognized as a promising material for its potential application in chemical sensors, transparent conductors, transparent UV protection films, catalysis and optoelectronic devices such as light-emitting devices, solar cells [5–15]. The noncentral symmetry of ZnO makes it piezoelectric. The unique semiconducting and piezoelectric dual property of ZnO makes it a promising multifunctional material and is utilized in the preparation of nanogenerator devices [16,17].

ZnO clusters of different particle sizes and morphologies have been synthesized by various physical and chemical techniques such as sol-gel method, gas-phase reaction, thermal decomposition and hydrothermal synthesis [18–26]. A few workers have reported the stability of small zinc oxide nanoclusters by observing distribution of zinc oxide nanostructures from a time-of-flight mass spectrometry initiated by laser ablation of solid zinc oxide [27–31]. Among the theoretical studies, there have been investigations for the structural stabilities, HOMO-LUMO gaps and optical absorption of some nanoclusters of Zn_iO_i type. However, other physical properties like the vibrational modes of stable nanoclusters of binary Zn_mO_n nanoclusters have not been reported so for up to the knowledge of authors. Mataxian *et al.* [32] have performed a TDDFT calculation for the excitation energies of optimized Zn_iO_i nanoclusters, which show a strong dependence on the geometry of nanoclusters. Wu *et al.* [33] have synthesized ZnO quantum dots by electroportation method and observed band gap oscillation.

[a] e-mail: psycmprl@rediffmail.com
[b] e-mail: pdhiraj2000@gmail.com

In this paper, we report normal modes of vibrations of most stable binary Zn_mO_n ($m+n = 2$ to 5) nanoclusters by using B3LYP-DFT/6-311G(3df) method. We have also calculated IR intensities, Rel IR intensities, Raman scattering activities and used the TDDFT formalism for determining the characteristic absorption spectra of these most stable nanoclusters. We have compared our predicted results with the other calculated and experimental results wherever available. In sect. 2, we present the method used in the investigations. Section 3 contains the calculation and results. The conclusions are contained in sect. 4.

2 Method

For the structural optimization of the ZnO nanoclusters, we have employed the B3LYP-DFT/6-311G(3df) version in the Gaussian-03 code (Gaussian 2003) [34] which employs the hierarchy of procedures corresponding to different approximation methods. The exact exchange in the Hartree-Fock theory for a single determinant is replaced in DFT by a more general expression, the exchange-correlation functional which includes terms accounting both for the exchange energy and the electron correlation.

In BLYP, we consider the Becke [35,36] exchange functional and the correlation function of Lee, Yang and Parr (LYP) [37,38] which includes both the local and nonlocal contributions. In B3LYP, we employ the three parameter hybrid functional of Becke. It may be noted that Becke functional considers the Slater exchange along with the corrections involving the gradient of the density.

A large basis set for each atom is selected for a most precise calculation. We use triple split valence basis set, 6-311G which employs three sizes of the contracted functions per orbital type. Contracted functions are the combination of Gaussian functions for the atomic orbitals. The advantage of the split valence basis set is that it allows the orbitals to change their size without making any change in the shape of the orbitals. For overcoming this limitation, one uses a polarizable basis set, 6-311G(3df) by adding orbitals with the angular momentum wherever necessary for the description of the ground state of each atom. For O and Zn atoms, we add three d functions and one f function, respectively. For generating quite accurate structural parameters, the triple zeta basis set and multiple polarization functions have been considered. The usual TDDFT formalisms have been considered for calculating the optical spectra.

3 Calculation and results

Different types of all possible structures including the linear chains, rings, planer and three-dimensional ones for each configuration have been considered in the optimization of ZnO nanoclusters. Each structure is achieved to its minimum energy by relaxing the atomic positions. The convergence in the system energy up to 10^{-7} meV and the forces of 10^{-3} eV/Å on each atom were obtained. A structure is said to be stable for which all the vibrational frequencies are real and none of them is imaginary. For similar values of "m" and "n" in Zn_mO_n, there are several structures for which all the vibrational frequencies are real. Among all the different atomic configuration of Zn_mO_n system, the configuration which possesses maximum binding energy is named as most stable structures.

3.1 Vibrational properties

We calculate the second derivatives of the total energy of the system with respect to the atomic displacements. The obtained dynamical matrix is diagonalized. We have also calculated the infrared intensities (IR int.), relative infrared intensities (Rel. IR int.) and Raman scattering activities (Raman Activity). The above calculated physical quantities for all the most stable nanoclusters are presented in table 1. In this table, the brackets following the frequencies denote the multiplicity of the mode. The above physical properties have not been studied by any other worker. All possible modes of vibrations of each most stable nanocluster of fig. 1 are presented in figs. 2–6. In the figures, the arrows indicate the direction and magnitude of the displacements of atoms during the different modes of vibration, while small displacement (below 0.10 Å) is neglected. We discuss the above properties of each nanocluster below.

ZnO

We obtain the stretching mode frequency (fig. 2(a)) of 401 cm^{-1} for ZnO nanocluster, while Wang *et al.* [39] have obtained it as 665 cm^{-1}. This stretching vibration is both IR and Raman-active.

Zn_mO_n $(m + n = 3)$

ZnO_2: For the linear OZnO configuration (fig. 1(b)), there are four normal modes of vibrations. The highest frequency of 863 cm^{-1} is obtained due to the asymmetric stretching vibration (fig. 2(d)) of the Zn and O atoms along

Table 1. The calculated vibrational frequencies in cm^{-1}, Infrared intensities (IR Int.) in KM Mol^{-1}, relative IR intensities (Rel. IR Int.) and Raman scattering activities (Raman activity) in A^4/AMU of the most stable Zn_mO_n ($m + n = 2$ to 5) configuration. Brackets following the frequencies contain the multiplicity of the mode.

Configuration	Properties	Values
Linear ZnO (1a)	Frequency	401
	IR Int.	0.06
	Rel. IR Int.	1.0
	Raman activity	37.62
Linear OZnO (1b)	Frequencies	183(2), 645, 863
	IR Int.	46.56, 0.00, 18.45
	Rel. IR Int.	1.00, 0.00, 0.40
	Raman activity	0.00, 70.18, 0.00
Triangular Zn_2O (1c)	Frequencies	95, 353, 500
	IR Int.	4.47, 5.24, 1.16
	Rel. IR Int.	0.85, 1.00, 0.22
	Raman activity	22.06, 31.85, 10.98
Rhombus ZnO_3 (1d)	Frequencies	189, 281, 304, 708, 923, 1088
	IR Int.	0.32, 6.61, 22.16, 3.54, 174.60, 4.58
	Rel. IR Int.	0.00, 0.04, 0.13, 0.02, 1.00, 0.03
	Raman activity	2.16, 0.03, 20.86, 24.31, 0.03, 22.09
Rhombus Zn_2O_2 (1e)	Frequencies	184, 220, 262, 467, 521, 592
	IR Int.	57.68, 0.00, 172.51, 0.00, 16.19, 0.00
	Rel. IR Int.	0.33, 0.00, 1.00, 0.00, 0.09, 0.00
	Raman activity	0.00, 14.22, 0.00, 0.49, 0.00, 7.91
Trigonal Zn_3O (1f)	Frequencies	23, 64, 71, 204, 492, 511
	IR Int.	23.39, 1.25, 1.46, 0.00, 0.93, 1.49
	Rel. IR Int.	1.00, 0.05, 0.06, 0.00, 0.04, 0.06
	Raman activity	0.00, 26.83, 27.15, 2.85, 34.89, 38.98
Pentagonal Zn_3O_2 (1g)	Frequencies	91, 101, 138, 199, 224, 562, 578, 636, 746
	IR Int.	0.00, 0.20, 3.76, 77.51, 2.54, 25.10, 81.53, 0.66, 6.05
	Rel. IR Int.	0.00, 0.00, 0.05, 0.96, 0.03, 0.31, 1.00, 0.00, 0.07
	Raman activity	0.86, 35.81, 9.03, 0.62, 10.69, 32.13, 18.38, 4.22, 18.06

the chain. The breathing vibrations (fig. 2(c)) of O atoms appear as the mid frequency of $645\,cm^{-1}$. The lowest doublet frequency of $183\,cm^{-1}$ corresponds to the bending vibration (fig. 2(b)). The lowest and highest frequency vibrations are infrared active but not Raman-active while the mid frequency vibration is Raman active but not infrared active.

Zn_2O: The Zn_2O triangular structure (fig. 1(c)) has three normal modes of vibrations. The asymmetric stretching vibration (fig. 2(g)) has the maximum frequency of $500\,cm^{-1}$, as where the breathing vibration (fig. 2(f)) has frequency, $353\,cm^{-1}$. The lowest frequency, $95\,cm^{-1}$ (fig. 2(e)) corresponds to the bending vibration of the cluster. All the vibrations are both IR-active and Raman-active.

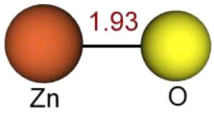

(a) ZnO Linear

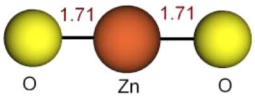

(b) ZnO_2 Linear

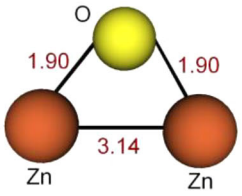

(c) Zn_2O Triangular

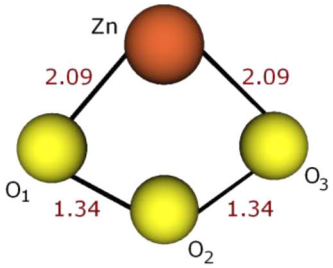

(d) ZnO_3 Rhombus

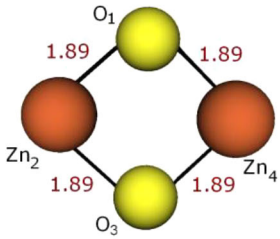

(e) Zn_2O_2 Rhombus

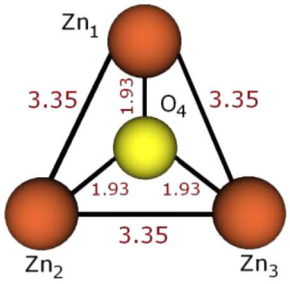

(f) Zn_3O Trigonal

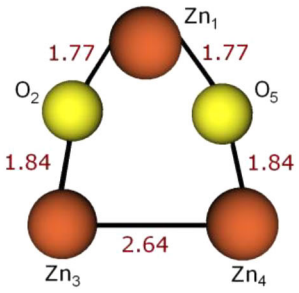

(g) Zn_3O_2 Pentagonal

Fig. 1. Most stable structures of Zn_mO_n $(m + n = 2$ to 5) nanoclusters.

Zn_mO_n $(m + n = 4)$

ZnO_3: For the rhombus ZnO_3 configuration (fig. 1(d)), there are six normal mode vibrational frequencies. The lowest frequency of 189 cm^{-1} arises due to asymmetric stretching vibration of Zn–O bonds (fig. 3(a)), while the highest frequency of 1088 cm^{-1} corresponds to the symmetric vibration of O–O bonds (fig. 3(f)). Other mid frequencies arise due to out of plane vibration (fig. 3(b)), symmetric stretching (fig. 3(c)) and asymmetric stretching (fig. 3(d), 3(e)) vibrations. Both the highest- and lowest-frequency vibrations are Raman-active.

Zn_2O_2: For the rhombus structure (fig. 1(e)), we again obtain six normal modes of vibratonal frequencies. The highest frequency of 592 cm^{-1} corresponds to the breathing vibrations (fig. 4(f)) of Zn and O atoms while the lowest frequency of 184 cm^{-1} arises due to out of plane vibration (fig. 4(a)) of Zn and O atoms. Other mid frequencies are for the asymmetric stretching vibrations (fig. 4(b), 4(c), 4(e)) and rocking vibration (fig. 4(d)). Some modes are either Raman-active or IR-active.

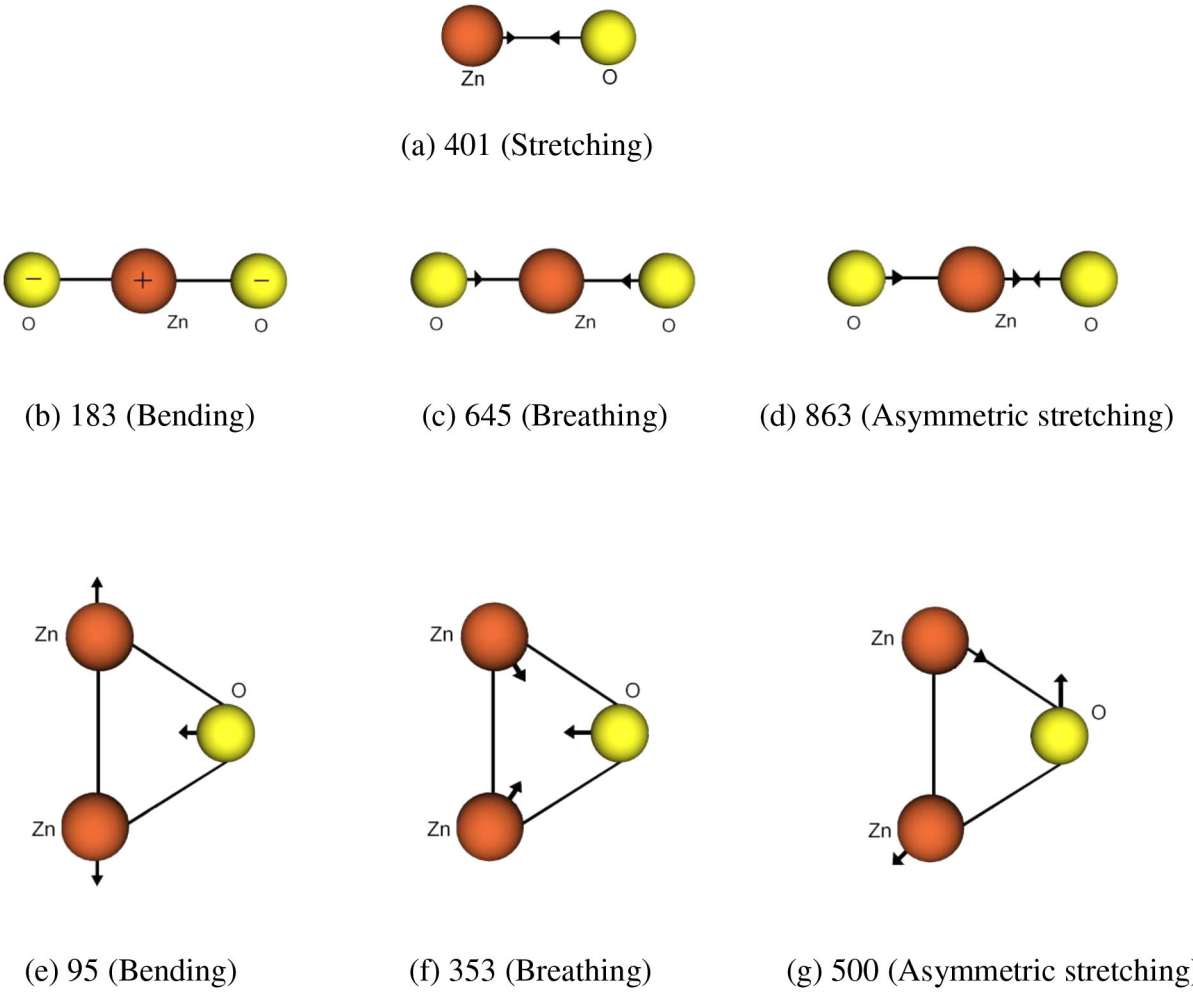

Fig. 2. Normal modes of vibrations of most stable ZnO linear, ZnO_2 linear and Zn_2O triangular nanoclusters. The numbers are the frequencies in cm^{-1}. The nature of vibration is given inside brackets.

Zn_3O: The trigonal Zn_3O configuration (fig. 1(f)) has six normal modes of vibrational frequencies. The low-lying frequency of $23\,cm^{-1}$ originates from the out of plane vibration of O atom while the frequency, $71\,cm^{-1}$ originates from the bending vibration (fig. 5(c)). The two mid frequencies, 204 and $492\,cm^{-1}$ arise due to breathing and stretching vibrations (fig. 5(d), 5(e)), respectively. All the vibrations are IR-active except the $204\,cm^{-1}$. One barring the vibration $23\,cm^{-1}$, all the vibrations are Raman-active.

$Zn_mO_n \quad (m+n=5)$

All the studied configurations of ZnO_4, Zn_2O_3 and Zn_4O complexes contain some imaginary frequencies and are thus unstable according to our definition of a stable structure.

Zn_3O_2: For the planer configuration of Zn_3O_2 complex, some calculated frequencies are found to be imaginary and therefore it as unstable. For the next structure having minimum energy *i.e.* pentagonal Zn_3O_2 structure (fig. 1(g)), there are nine normal modes of vibrational frequencies. The highest frequency of $746\,cm^{-1}$ originates from asymmetric stretching vibration. The frequencies, 91 and $199\,cm^{-1}$ correspond to the out of plane vibrations (fig. 6(a), 6(d)) of Zn and O atoms. All others frequencies arise due to stretching, and bending vibrations. Further, most of the vibrations are IR-active and Raman-active.

The above study of the different vibrations of the different structures shows that the high vibrational frequencies arise from the symmetrical and asymmetrical stretching vibrations. The lower frequencies belong to the wagging, rocking and the out of plane vibrations of Zn and O atoms. The above discussion also reveals that the nanoclusters of ZnO_4, Zn_2O_3 and Zn_4O configurations are unstable, as all or some their frequencies are found to be imaginary. We also found that although the planer Zn_3O_2 structure has minimum energy but as its vibrational frequencies are found to be imaginary, it is unstable.

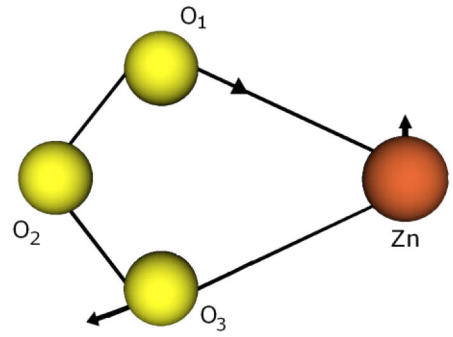

(a) 189 (Asymmetric stretching)

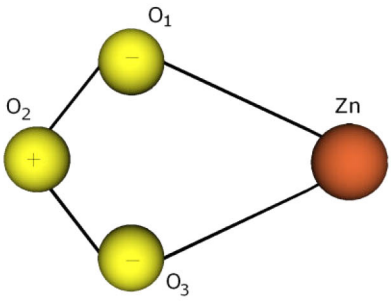

(b) 281 (Out of plane vibration)

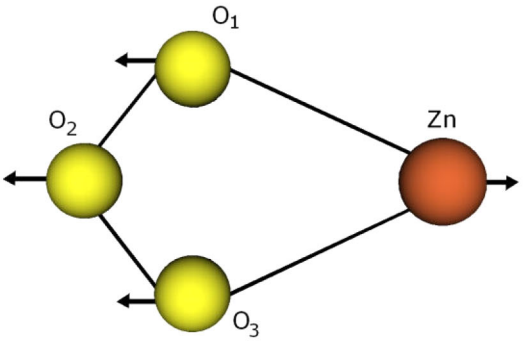

(c) 304 (Symmetric stretching)

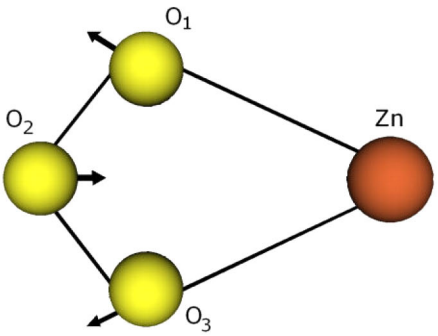

(d) 708 (Asymmetric stretching)

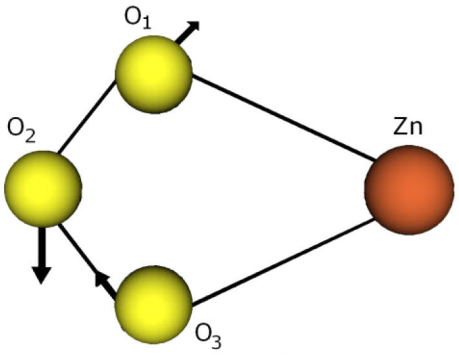

(e) 923 (Asymmetric stretching)

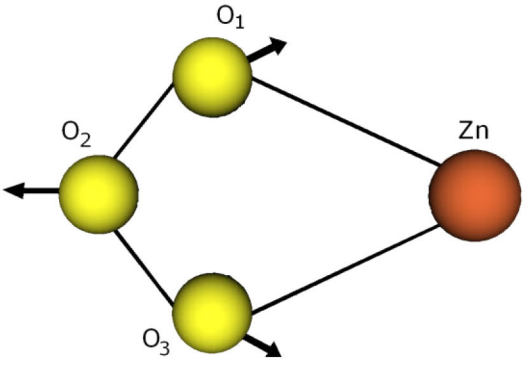

(f) 1088 (Symmetric stretching)

Fig. 3. Normal modes of vibrations of most stable ZnO_3 rhombus nanocluster. The numbers are the frequencies in cm^{-1}. The nature of vibration is given inside brackets.

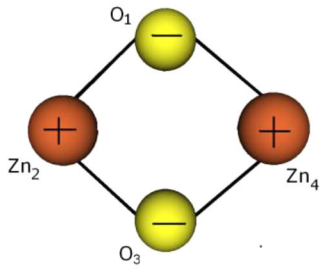

(a) 184 (Out of plane Vibration)

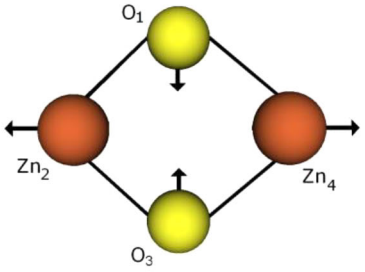

(b) 220 (Asymmetric stretching)

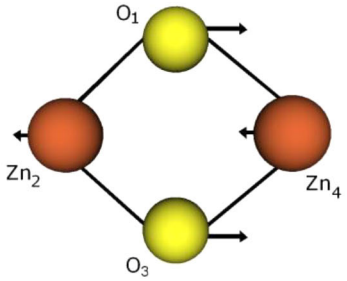

(c) 262 (Asymmetric stretching)

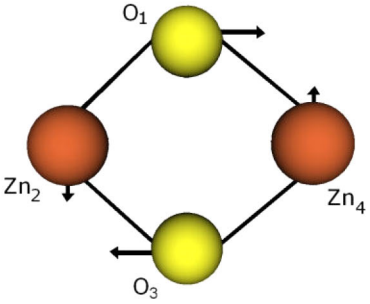

(d) 466 (Rocking)

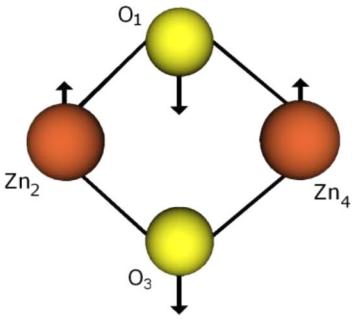

(e) 521(Asymmetric stretching)

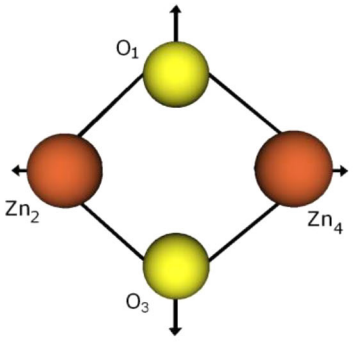

(f) 592 (Breathing)

Fig. 4. Normal modes of vibrations of most stable Zn_2O_2 rhombus nanocluster. The numbers are the frequencies in cm^{-1}. The nature of vibration is given inside brackets.

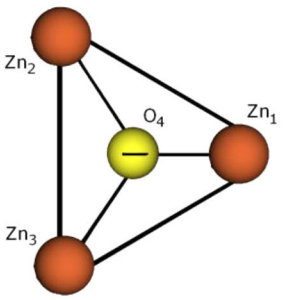

(a) 23 (Out of plane vibration)

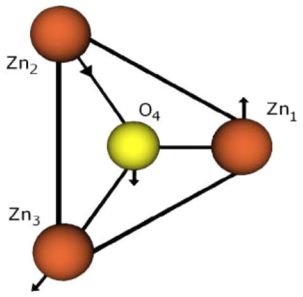

(b) 64

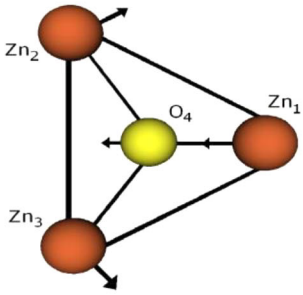

(c) 71 (Bending)

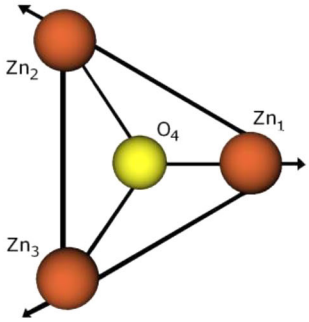

(d) 204 (Breathing)

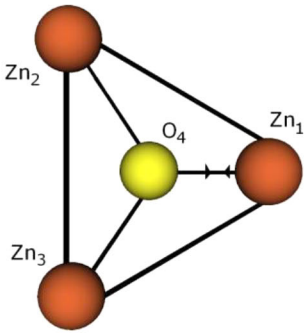

(e) 492 (Stretching)

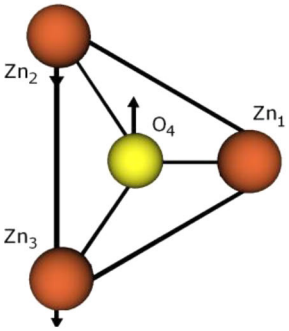

(f) 511 (Asymmetric stretching)

Fig. 5. Normal modes of vibrations of most stable Zn_3O trigonal nanocluster. The numbers are the frequencies in cm^{-1}. The nature of vibration is given inside brackets.

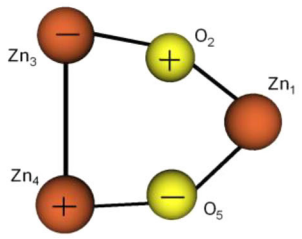

(a) 91 (Out of plane vibration)

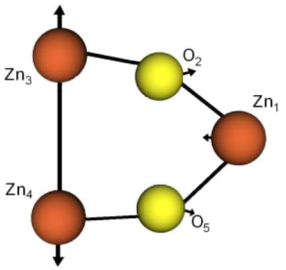

(b) 101 (Bending)

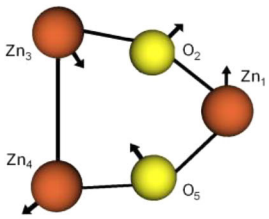

(c) 138

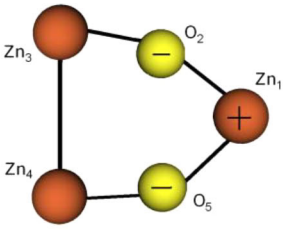

(d) 199 (Out of plane vibration)

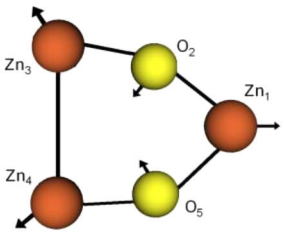

(e) 224 (Breathing)

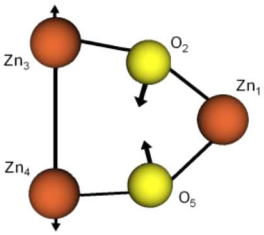

(f) 562 (Asymmetric stretching)

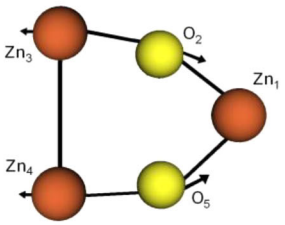

(g) 578 (Symmetric stretching)

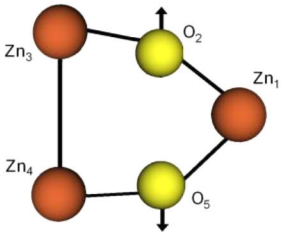

(h) 636 (Stretching)

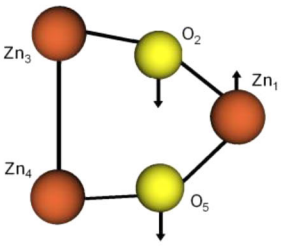

(i) 746 (Asymmetric stretching)

Fig. 6. Normal modes of vibrations of most stable Zn_3O_2 pentagonal nanocluster. The numbers are the frequencies in cm^{-1}. The nature of vibration is given inside brackets.

3.2 Optical properties

We present the calculated optical absorption spectra, which will be similar to the electron energy loss spectra (EELS) in figs. 7 and 8. In most of the nanoclusters, the absorption spectrum is strong in the ultraviolet region but in a few configurations one observes weak absorption in the visible region. The minimum excitation energies having the largest oscillator strengths for the most stable Zn_mO_n nanoclusters are compared with the available experimental data in table 2. One observes an excellent agreement with the available experimental data. Now the absorption spectra of each nanocluster is discussed below.

ZnO

For the simplest diatomic nanocluster (fig. 1(a)), the calculated absorption region is shown in fig. 7(a). A strong peak appears at 5.27 eV which is very close to the experimental observed value of 5.66 eV [33]. There also appears a very weak peak at 8.89 eV.

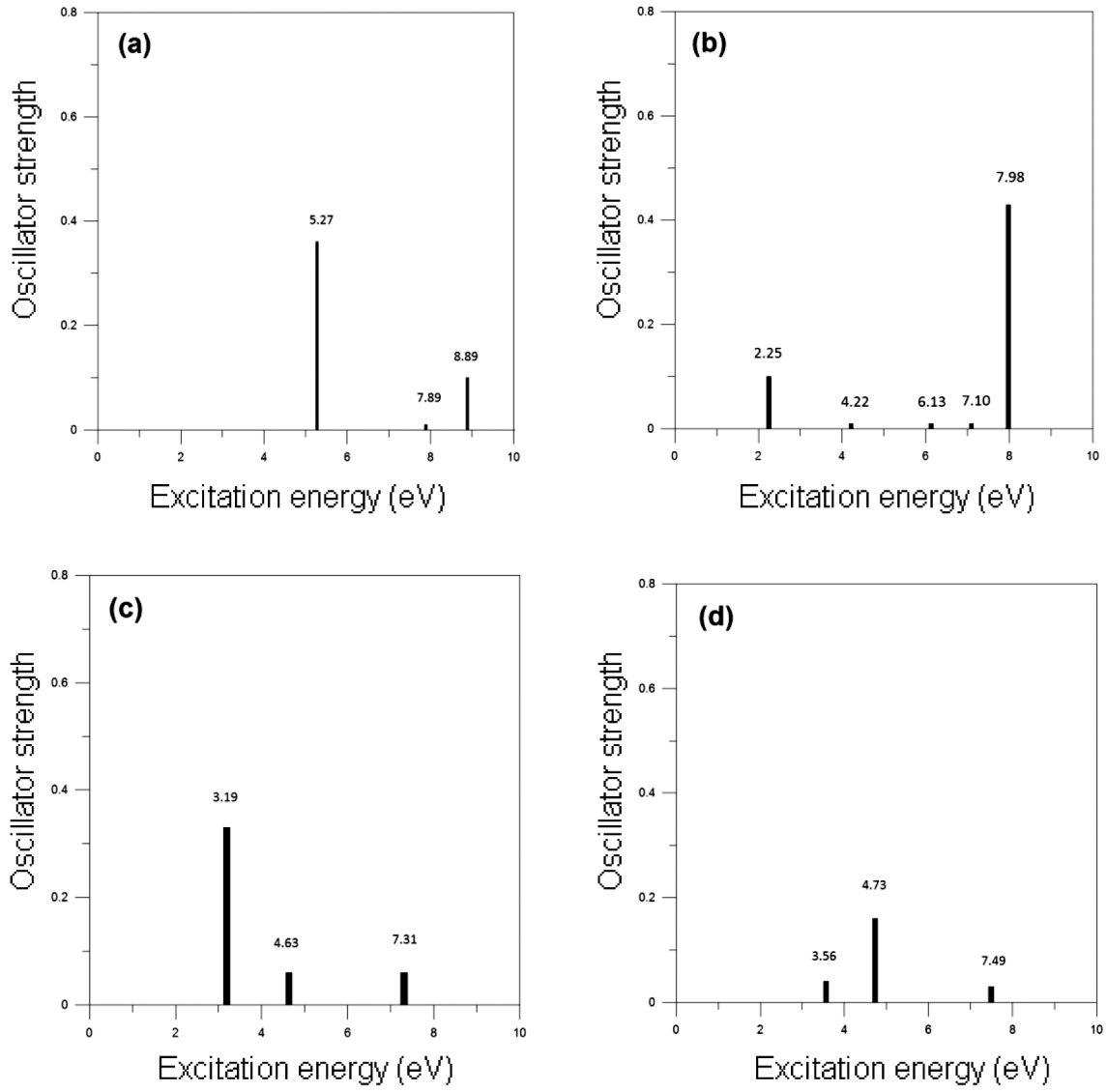

Fig. 7. Absorption spectra for the most stable structures of (a) linear ZnO (b) linear ZnO_2 (c) triangular Zn_2O and (d) rhombus ZnO_3.

Zn_mO_n $(m+n=3)$

In the case of the linear OZnO nanocluster (fig. 1(b), very strong sharp peak appears at 7.98 eV corresponding to the minimum excitation energy (fig. 7(b)).

For the triangular Zn_2O nanocluster (fig. 1(c)), one observes a strong absorption peak at 3.19 eV in the upper side of the visible region. It corresponds to the minimum energy excitation. Quite weak absorption is seen in other region of energy (fig. 7(c)).

Zn_mO_n $(m+n=4)$

For the rhombus ZnO_3 (fig. 1(d)) configuration, a strong absorption is seen at 4.73 eV. Some absorption is also seen at 3.56 and 7.49 eV.

For the rhombus Zn_2O_2 (fig. 1(e)) complex, weak absorption appears at the infrared region 1.14 eV and strong absorption is seen in the ultraviolet region. Comparable strong absorption occurs in the energy range 4.30–5.90 eV as shown in fig. 8(a). The strong absorption peak appearing at 5.04 eV is very close to the experimentally observed value of 5.19 eV [33].

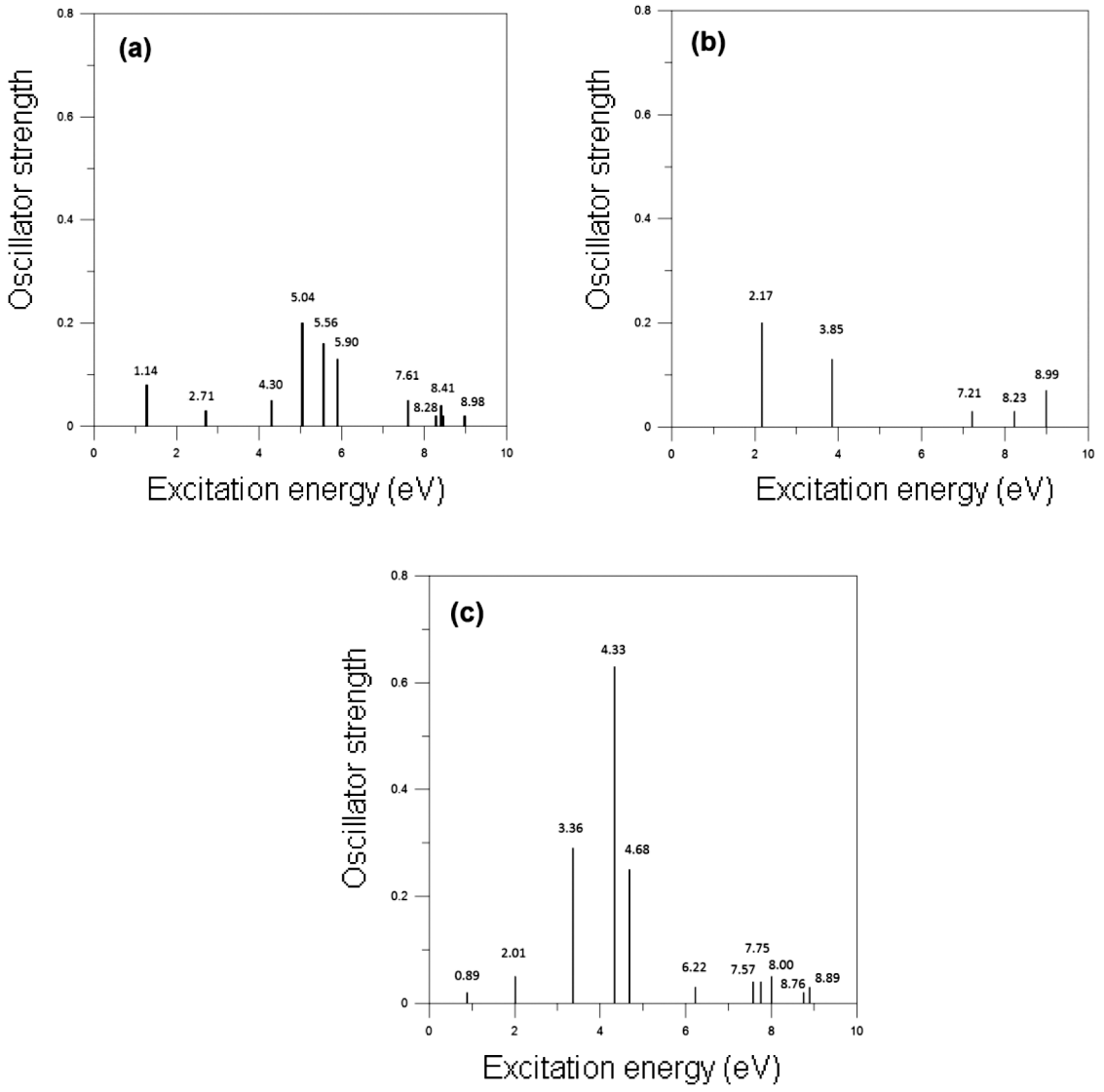

Fig. 8. Absorption spectra for the most stable structures of (a) rhombus Zn_2O_2 (b) trigonal Zn_3O and (c) pentagonal Zn_3O_2.

In the absorption spectra of the trigonal Zn_3O (fig. 1(f)) configuration, two strong peaks appear at 2.17 eV and 3.85 eV. These peaks correspond to the excitation energies of the cluster. Weak absorption is seen in the ultraviolet region.

$Zn_mO_n \quad (m+n=5)$

In the absorption spectra of the pentagonal Zn_3O_2 structure (fig. 1(g)), three sharp peaks are seen corresponding to the various excitation energies. These strong peaks appear at 3.36, 4.33 and 4.68 eV as depicted in fig. 8(c). Weak absorption also appears in the other parts of the energy region.

Most of the nanoclusters show strong absorption in the ultraviolet region but few nanoclusters like linear ZnO, linear ZnO_2, trigonal Zn_3O and pentagonal Zn_3O_2 exhibit absorption in the visible region also.

4 Conclusion

This study presents the vibrational and optical properties of the most stable structures up to five atom ZnO nanoclusters. We predict the vibrational frequencies, IR intensity, Rel IR intensity and Raman scattering activities and optical properties which need to be verified experimentally.

For $m+n=5$, we found that only Zn_3O_2 configuration is stable. On the other hand, ZnO_4, Zn_2O_3 and Zn_4O configurations have no stable structure as all the investigated structures of these configurations have at least one imaginary vibrational frequency. The above study shows that the high vibrational frequencies arise from the symmetrical

Table 2. Excitation energies (ΔE, in eV) having largest oscillator strengths (f) for the most stable configurations of Zn_mO_n ($m+n=2$ to 5) nanoclusters.

Nanocluster	Configuration	Excitation energy (ΔE, in eV)		Oscillator strength (f)
		Present	Experimental	
ZnO	Linear ZnO (1a)	5.27	5.66	0.36
ZnO_2	Linear OZnO (1b)	7.98		0.43
Zn_2O	Triangular (1c)	3.19		0.33
ZnO_3	Rhombus (1d)	4.73		0.16
Zn_2O_2	Rhombus (1e)	5.04	5.19	0.20
Zn_3O	Trigonal (1f)	2.17		0.20
Zn_3O_2	Pentagonal (1g)	4.33		0.63

and asymmetrical stretching vibrations whereas the lower frequencies belong to wagging, rocking and the out of plane vibrations of Zn and O atoms. Our calculated results for the excitation energies of Linear ZnO and Rhombus Zn_2O_2 nanoclusters exhibit close agreement with the experimental data as shown in table 2. Almost all the nanoclusters show strong absorption in the ultraviolet region. Some nanoclusters show appreciable absorption in the visible region.

The authors are thankful to University Grants Commissions, New Delhi for its financial assistance.

References

1. E.R. Bernstien (Editor), *Atomic and Molecular Clusters Studies in Physical and Theoretical Chemistry*, Vol. **68** (Elsevier, Amsterdam, 1990).
2. P. Jena, B.K. Rao, S.N. Khanna, *Physics and Chemistry of Small Clusters*, *NATO ASI Ser.*, Vol. **158**, (Kluwer, Dordrecht, 1990).
3. H.J. Himmel, N. Hebben, Chem. Eur. J. **11**, 4096 (2005).
4. S.M. Sheehan, G. Meloni, B.F. Parsons, N. Wehres, D.M. Neumark, J. Chem. Phys. **124**, 064303 (2006).
5. Z.L. Wang, X.Y. Kong, Y. Ding, P.X. Gao, W.L. Hughes, R.S. Yang, Y. Zhang, Adv. Funct. Mater. **14**, 943 (2004).
6. Z.L. Wang, Mater. Today **7**, 26 (2004).
7. Z.K. Tang, G.K.L. Wang, P. Yu, M. Kawasaki, A. Ohtomo, H. Koinuma, Y. Segawa, Appl. Phys. Lett. **72**, 3270 (1998).
8. J.H. Choy, E.S. Jang, J.H. Won, J.H. Chung, D.J. Jang, Y.W. Kim, Adv. Funct. Mater. **15**, 1911 (2003).
9. H. Kind, H. Yan, M. Law, B. Messer, P. Yang, Adv. Mater. **14**, 158 (2002).
10. Z.R. Dai, Z.W. Pan, Z.L. Wang, Adv. Funct. Mater. **13**, 9 (2003).
11. S. Saito, M. Miyayama, K. Koumoto, J. Am. Ceram. Soc. **68**, 40 (1985).
12. S.J. Pearton, D.P. Norton, K. Ip, Y.W. He, T. Steiner, Prog. Mater. Sci. **50**, 293 (2005).
13. B.S. Jeon, J.S. Yoo, J.D. Lee, J. Electrochem. Soc. **143**, 3923 (1996).
14. P.L. Hower, T.K. Gupta, J. Appl. Phys. **50**, 4847 (1979).
15. W.G. Morris, J. Vac. Sci. Technol. **13**, 926 (1976).
16. Z.L. Wang, J. Phys. Condens. Matter **16**, 829 (2004).
17. Z.L. Wang, J. Song, Science **312**, 242 (2006).
18. J. Antony, X.B. Chen, J. Morrison, L. Bergman, Y. Qiang, Appl. Phys. Lett. **87**, 241917 (2005).
19. K.S. Choi, H.C. Lichtenegger, G.D. Stucky, J. Am. Chem. Soc. **124**, 12402 (2002).
20. S. Maensiri, P. Laokul, V. Promarak, J. Cryst. Growth **289**, 102 (2006).
21. C. Wu, X. Qiao, J. Chen, H. Wang, F. Tan, S. Li, Mater. Lett. **60**, 1828 (2006).
22. M. Li., H. Bala, X. Lv, X. Ma, F. Sun, L. Tang, Z. Wang, Mater. Lett. **61**, 690 (2007).
23. W.J. Li, E.W. Shi, W.Z. Zhong, Z.W. Yin, J. Cryst. Growth **203**, 186 (1999).
24. K.H. Tam, C.K. Cheung, Y.H. Leung, A.B. Djurisic, C.C. Ling, C.D. Beling, S. Fung, W.M. Kwok, W.K. Chan, D.L. Phillips, L. Ding, W.K. Ge, J. Phys. Chem. B **110**, 20865 (2006).
25. Z. Fan, J.G. Lu, J. Nanosci. Nanotechnol. **5**, 1561 (2005).
26. Z.L. Wang, J. Phys.: Condens. Matter **16**, 829 (2004).
27. D. Cannavo, G. Knopp, P. Radi, P. Beaud, M. Tulej, P. Bodek, T. Gerber, A. Wokaun, J. Mol. Struct. **782**, 67 (2006).

28. A. Burnin, J.J. BelBruno, Chem. Phys. Lett. **362**, 341 (2002).
29. A.V. Bulgakov, I. Ozerov, W. Marine, *Laser ablation synthesis of zinc oxide clusters: a new family of fullerenes?* arXiv:physics/0311117 (2003).
30. L.M. Kukreja, A. Rohlfing, P. Misra, F. Hillenkamp, K. Dreisewerd, Appl. Phys. A: Mater. Sci. Process **78**, 641 (2004).
31. A. Dmitruk, I. Dmitruk, I. Blonsky, R. Belosludov, Y. Kawazoe, A. Kasuya, Microele. J. **40**, 218 (2009).
32. J.M. Matxain, J.M. Mercero, J.E. Fowler, J.M. Ugalde, J. Am. Chem. Soc. **125**, 9494 (2003).
33. S. Wu, N. Yuan, H. Xu, X. Wang, Z.A. Schelly, Nanotechnology **17**, 4713 (2006).
34. Gaussian, Inc. (2003) *GAUSSIAN 03*, Revision C.03 (Pittsburgh, PA: Gaussian).
35. A.D. Becke, J. Chem. Phys. **98**, 5648 (1993).
36. A.D. Becke, Phys. Rev. A **38**, 3098 (1988).
37. C. Lee, W. Yang, R.G. Parr, Phys. Rev. B **371**, 785 (1988).
38. B. Miehlich, A. Savin, H. Stoll, H. Preuss, Chem. Phys. Lett. **157**, 200 (1989).
39. B. Wang, S. Nagas, J. Zhao, G. Wang, J. Phys. Chem. C **111**, 4956 (2007).